

Influence of jet discharge velocity profile on CFD simulation of pump-around jet mixing tank

Thanwa Jorakit¹, Natthanon Phaiboonsilpa¹, Apinan Namkanisorn¹, Phisan Ponpo¹, Eakarach Bumrungthaichaichan¹, and Santi Wattananusorn^{1,*}

¹Department of Chemical Engineering, Faculty of Engineering, King Mongkut's Institute of Technology Ladkrabang, Bangkok, Thailand

Abstract. The present paper shows the effect of jet discharge velocity profile (or jet nozzle configuration) on CFD simulation of an open 45° inclined side entry pump-around jet mixing tank. The CFD model was carefully developed by using appropriate grid arrangement, boundary conditions, and numerical methods. The two different jet discharge velocity profiles, including top hat and fully developed profiles, were simulated by using the inlet mass flow rate of about 0.22 kg·s⁻¹. The overall mixing times and normalized concentration profiles predicted by two different jet discharge velocity profiles were compared with the previous reliable experimental data. The results revealed that the different jet discharge velocity profiles resulted in different jet flow and mixing patterns inside the vessels.

1 Introduction

Jet mixing tank is a mixing device that uses high velocity liquid jet to mix the different components inside the vessel. It was firstly introduced by Fossett and Prosser [1] in 1949. Nowadays, it becomes an important mixing device because of various advantages, including simple design with non-moving part, inexpensive operating cost, and easy installation and maintenance.

Over 60 years or so, the different jet mixing time correlations were obtained by experiments. However, the universal mixing time correlation was unavailable. That is, these correlations predicted the overall mixing times well only for the range of studied parameters, i.e. these correlations were case specific [2]. Moreover, the details of fluid flow and mixing inside the vessel were not presented. So, the computational fluid dynamics (CFD) has been employed to address these problems.

One of the earliest CFD studies on jet mixing tank has been carried out by Brooker [3]. He revealed that his CFD model well predicted the overall mixing time with the maximum error of about 15% as compared to the experimental data. Later, the effects of jet mixing tank configurations and operating conditions, such as jet elevation, jet angle, tank shape, liquid height, jet injection rate, etc., on jet mixing behaviour were studied. Further, the effects of turbulence model and numerical methods on mixing behaviour were also investigated. However, the influence of jet discharge velocity profile (or jet nozzle configuration), which directly affects on jet flow pattern inside the vessels, was not represented.

Generally, for round jet, the different jet nozzle configurations provide the different jet discharge velocity profiles. The jet discharge velocity profiles of

smooth contraction nozzle (SC) and long pipe nozzle (LP) respectively are top hat (TH) and fully developed (FD), which is generally described by one-seventh-power law. For constant inlet mass flow rate, the discharge velocity profiles of SC and LP are shown in Fig. 1. Further, these different nozzle geometries also represent the different jet flow patterns. For SC, the jet potential core length is about 4-6 nozzle diameter (d_j). Whereas, the potential core region of LP is not observed.

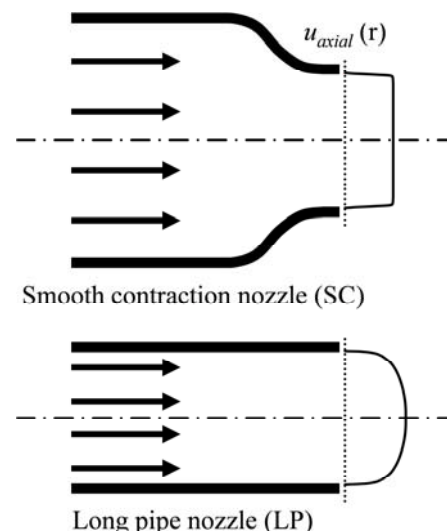


Fig. 1. Jet discharge velocity profiles of SC and LP

So, in this work, the two different jet discharge velocity profiles, including TH and FD, were simulated to investigate the jet flow pattern and mixing behaviour inside the open 45° inclined side entry pump-around jet mixing tank.

* Corresponding author: cfddgroup_santi@hotmail.com

2 Description of CFD modelling

2.1. Jet mixing tank

An open 45° inclined side entry pump-around jet mixing tank of Patwardhan [4] was employed to study the effect of jet discharge velocity profile. The diameter of flat bottom cylindrical tank was 0.5 m. The tap water height was 0.5 m. The diameter of jet nozzle and tank outlet pipe respectively were 0.008 m and 0.0381 m. The schematic of pump-around jet mixing tank is shown in Fig. 2.

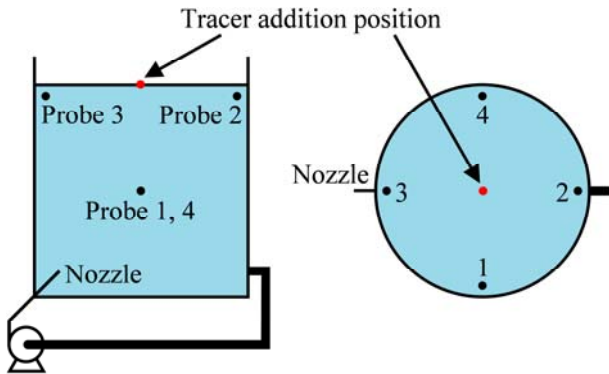


Fig. 2. Schematic of pump-around jet mixing tank

2.2 Grid generation

The GAMBIT 2.4.6 program was adopted to perform the three-dimensional solid model and grid generation of an open 45° inclined side entry pump-around jet mixing tank. The hexahedral grids were carefully generated inside the vessel to achieve the accurate results. That is, the grids were controlled to align with the flow direction to reduce the numerical errors by using the domain decomposition technique. Generally, in GAMBIT 2.4.6, the domain decomposition facility is unavailable. Thus, in order to use this technique, the jet mixing tank domain was manually split by using the specified faces. The grid generation of this mixing tank is shown in Fig. 3.

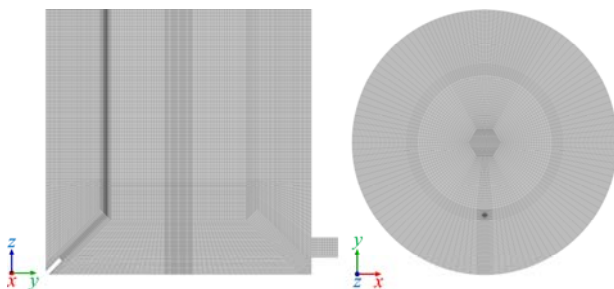


Fig. 3. Grid generation of pump-around jet mixing tank

2.3 Governing equations

For CFD simulation of jet mixing tank, the steady state flow pattern and turbulence field were obtained by using the Reynolds average equations for conservation of mass and momentum together with the realizable k-epsilon turbulence model (RKE). The compact form of steady state Reynolds average equation can be written as:

$$\frac{\partial(\rho U \phi)}{\partial x_j} = \frac{\partial}{\partial x_j} \left(\Gamma_\phi \frac{\partial \phi}{\partial x_j} \right) + S_\phi \quad (1)$$

where U is mean velocity vector, ϕ is a universal dependent variable, Γ_ϕ is the diffusivity, and S_ϕ is the source term. Further, the details of variables for continuity equation, momentum equation, and RKE are represented in Table 1.

Table 1. Variables for continuity equation, momentum equation and RKE [5]

Equation	ϕ	Γ_ϕ	S_ϕ
Continuity	1	0	0
Momentum	U_i	μ	$-\frac{\partial P}{\partial x_i} + \frac{\partial}{\partial x_j} \left(\mu_t \frac{\partial U_i}{\partial x_j} \right) + S_{M,i}$
k -transport	k	$\mu + \frac{\mu_t}{\sigma_k}$	$G_k + G_b - \rho \varepsilon - Y_M + S_k$
ε -transport	ε	$\mu + \frac{\mu_t}{\sigma_\varepsilon}$	$\rho C_1 S \varepsilon - \rho C_2 \frac{\varepsilon^2}{k + \sqrt{v \varepsilon}} + C_{1\varepsilon} \frac{\varepsilon}{k} C_{3\varepsilon} G_b + S_\varepsilon$

For jet mixing time investigation, the unsteady state species transport equations without chemical reaction [5] were iteratively solved and can be written as:

$$\frac{\partial(\rho Y_i)}{\partial t} + \frac{\partial(\rho U Y_i)}{\partial x_j} = \frac{\partial}{\partial x_j} \left(\left(\rho D_{i,m} + \frac{\mu_t}{Sc_t} \right) \frac{\partial Y_i}{\partial x_j} \right) + S_i \quad (2)$$

where Y_i is the local mass fraction of species i , $D_{i,m}$ is the mass diffusion coefficient for species i in the mixture, Sc_t is turbulent Schmidt number, μ_t is the eddy viscosity, and S_i is the source term for species transport equations.

Further, in order to evaluate the mixing time, the 95% mixing time was used. Generally, the 95% mixing time is the time required for concentration (c) to reach within 95% of the fully mixed value (\bar{c}) and can be written as:

$$t_{95\%} = \text{time for } \left| \frac{c - \bar{c}}{\bar{c}} \right| \leq 0.05 \quad (3)$$

Finally, the arithmetic average of mixing times obtained by four different probe locations was adopted to achieve the overall mixing time.

2.4. Boundary conditions

For steady state simulation, the velocity-inlet and pressure-outlet boundary condition types were adopted at inlet and outlet, respectively. Whereas, for unsteady state simulation, the recirculation-inlet and recirculation-outlet were used [6]. At inlet, the two different jet discharge velocity profiles with constant inlet mass flow

rate of about $0.22 \text{ kg}\cdot\text{s}^{-1}$ were specified. Moreover, for turbulence quantities, the turbulence kinetic energy of $0.2904 \text{ m}^2\cdot\text{s}^{-2}$ and its dissipation rate of $22.35614 \text{ m}^2\cdot\text{s}^{-3}$ were directly imposed. The no-slip boundary condition and standard wall functions were adopted at the tank wall. Further, the symmetry boundary condition was used at the top liquid surface.

Furthermore, the uniform inlet velocity of $4.4 \text{ m}\cdot\text{s}^{-1}$ was imposed at inlet for TH. For FD, the fully developed profile was obtained by preliminary CFD simulation of turbulent flow in circular pipe. The pipe diameter was 0.008 m . The pipe length was extended to 70 pipe diameter to ensure that the fully developed pipe flow was achieved. Then, the velocity profile at pipe outlet was extracted and written in C language as the user defined function (UDF). Finally, this UDF was specified at jet nozzle discharge section. The jet discharge velocity profiles for TH and FD are represented in Fig. 4.

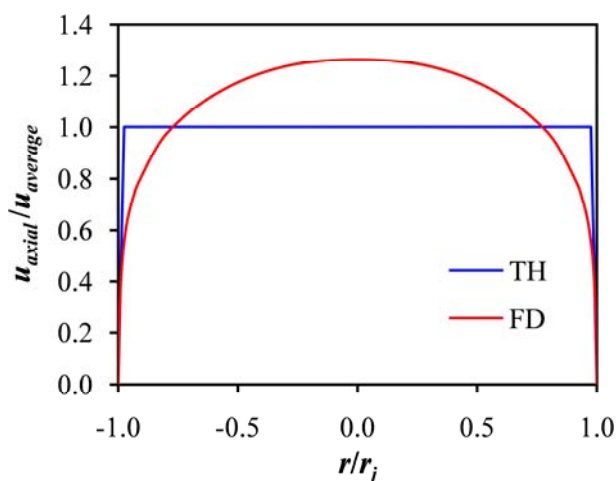


Fig. 4. Jet discharge velocity profiles (r_j is jet nozzle radius)

2.5. Numerical methods

For this work, the double precision pressure-based solver of ANSYS FLUENT program was employed to simulate pump-around jet mixing tank. The pressure-velocity coupling scheme, spatial discretization scheme, and temporal discretization scheme were SIMPLE, second order upwind, and first order implicit, respectively.

2.6. Solution strategy

The area weighted average of the velocity magnitude at plane $x = 0$ was monitored until it was constant to obtain the converged solutions of steady state simulation. For unsteady state simulation, the scaled residual of 10^{-5} for tracer was used as a convergence criterion. Further, the time step size of transient simulation was 0.0025 s [6, 7].

Moreover, the velocity magnitude gradient adaption with the refine threshold of 10% of the maximum value [8] was used to obtain the grid independent solutions. In order to obtain the grid independent solutions, the final grids of these models were achieved by adapting the grids three times as suggested by Bumrunthaichaichan et al. [6].

3 Results and discussion

In this work, the two different jet discharge velocity profiles, including TH and FD, were simulated to study the flow pattern and mixing behaviour inside an open 45° inclined side entry pump-around jet mixing tank. The predicted overall mixing times and normalized concentration profiles were compared with the results of Patwardhan [4] as represented in Table 2 and Fig. 5, respectively. Generally, the normalized concentration is defined as a ratio of the tracer concentration to the fully mixed value. Moreover, the jet axial velocity contours of two different jet discharge velocity profiles are shown in Fig. 6.

Table 2. Comparison of overall mixing times

Model	Mixing time [s]	% Error ^a
EXP [4]	31.00	-
TH	28.19	9.06
FD	25.27	18.48

^a The percentage error is a ratio of absolute difference between the predicted overall mixing time and experimental mixing time to the experimental value.

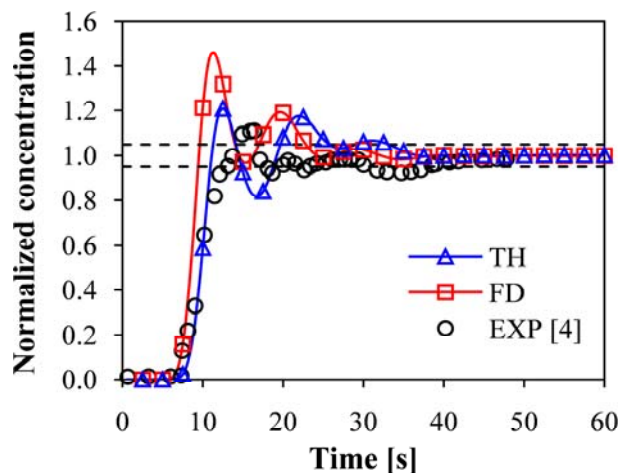


Fig. 5. Normalized concentration profiles at probe 1 (Note: The information of nozzle configuration of Patwardhan [4] was not reported)

From Table 2, the simulated results reveal that the predicted overall mixing times of TH and FD are lower than actual experiment. The percentage errors of TH and FD are about 9% and 18.5%, respectively. Further, the predicted overall mixing time of TH is higher than that predicted by FD, which indicates that the momentum available for mixing (convective transport) of FD is greater than that obtained by TH.

In Fig. 5, the results show that the normalized concentration profiles predicted by two different jet discharge velocity profiles are different. The start of normalized concentration profile obtained by FD is faster than that obtained by TH and the first peak value of normalized concentration profile for FD is higher than

that simulated by TH. The start and first peak values of these predicted normalized concentration profiles are respectively faster and higher than experimental data because of the overprediction in convective transport [6]. However, these predicted normalized concentration profiles approach the experimental profile at the large times.

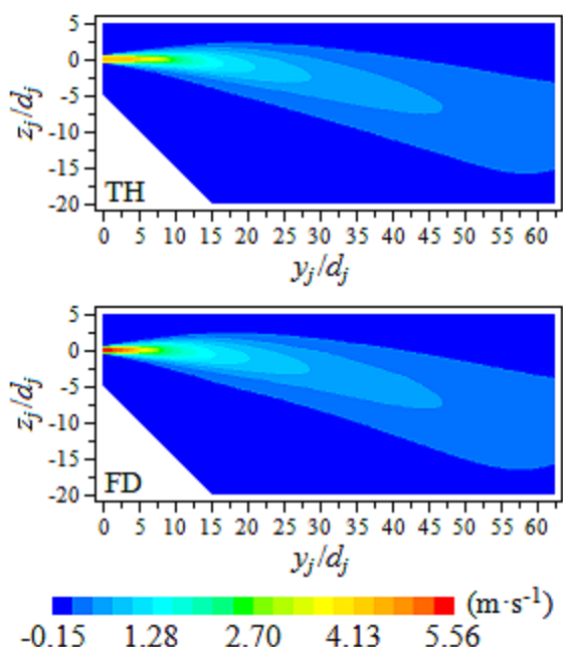


Fig. 6. Contours of jet axial velocity at plane $x = 0$ (y_j and z_j are jet longitudinal and jet radial distances.)

Fig. 6 shows the contours of axial velocity predicted by TH and FD. The results show that the axial velocities of TH and FD are found to decrease with increasing the longitudinal distance, which are similar to the general experiments of turbulent round jets [9]. For $y_j/d_j \leq 10$, the decay of centreline axial velocity of FD is faster than TH. For higher values of y_j/d_j , the decay of centreline axial velocity of two different jet discharge velocity profiles are slightly different. Further, the jet spreading of FD is slightly wider than TH, especially for y_j/d_j of about 12. This wider jet spreading of FD provides the higher convective transport as compared to the TH, which directly results in lower predicted overall mixing time.

According to these results, it can be seen that the overall mixing times predicted by TH and FD are lower than that obtained experimentally because these models overpredict the convective transport due to flat top liquid surface assumption [6]. Further, even when the jet inlet mass flow rate of TH and FD are identical, the different jet discharge velocity profiles represent the different jet flow and mixing patterns inside the vessels. Thus, the jet discharge velocity profile should be considered as another important parameter for developing the CFD model and mixing time correlation.

4 Conclusion

In this work, the effect of jet discharge velocity profile on jet flow pattern and mixing behaviour inside the pump-around jet mixing tank was numerically studied by considering the top hat (TH) and fully developed (FD) profiles. The overall mixing times and normalized concentration profiles predicted by two different jet discharge velocity profiles were compared with the measured data of Patwardhan [4]. The results revealed that even when the jet inlet mass flow rates of these CFD models were identical, the different jet discharge velocity profiles represented the different jet flow and mixing patterns inside the jet mixing vessels. That is, the different mixing patterns inside the tanks were directly affected by the different jet flow phenomena, such as decay of centreline velocity, jet spreading, etc. Further, the different jet flow characteristics of two discharge velocity profiles were caused by the differences in flow structures as reported by Xu and Antonia [9]. Hence, another important parameter for developing CFD model and mixing time correlation of pump-around jet mixing tank would be jet discharge velocity profile.

The authors would like to thank College of Advanced Manufacturing Innovation, King Mongkut's Institute of Technology Ladkrabang, Thailand for supporting the ANSYS FLUENT software.

References

1. H. Fossett, L.E. Prosser, Proc. I. Mech. E. **160**, 224 (1949)
2. E. Bumrunghthaichaihan, Korean J. Chem. Eng. **33**(11), 3050 (2016)
3. L. Brooker, Chem. Eng. **30**, 16 (1993)
4. A.W. Patwardhan, Chem. Eng. Sci. **57**, 1307 (2002)
5. ANSYS Inc., *ANSYS Fluent Theory Guide: Release 15.0* (ANSYS Inc., USA, 2013)
6. E. Bumrunghthaichaihan, A. Namkanisorn, S. Wattananusorn, J. Chin. Inst. Eng. (to be published)
7. E. Bumrunghthaichaihan, N. Jaiklom, A. Namkanisorn, S. Wattananusorn, Sci. Res. Essays **11**(4), 42 (2016)
8. ANSYS Inc., *ANSYS Fluent Tutorial Guide: Release 15.0* (ANSYS Inc., USA, 2013)
9. G. Xu, R.A. Antonia, Exp. Fluids **33**(5), 677 (2002)